Electronic Supplementary Material (ESI) for Nanoscale.

Supporting Information

Morphological and Structural Design Through Hard-Templating of PGM-Free Electrocatalysts for AEMFC Applications

Hilah C. Honig[+],[a] Silvia Mostoni[+],[b] Yan Presman,[a] Rifael Z. Snitkoff-Sol,[a] Paolo Valagussa,[b] Massimiliano D'Arienzo,[b] Roberto Scotti,[b,c] Carlo Santoro,[b] Mohsin Muhyuddin*,[b] Lior Elbaz [a]**

[a] Chemistry Department, Bar-Ilan Center for Nanotechnology and Advanced Materials, Bar-Ilan University, Ramat-Gan 5290002, Israel.

[b] Department of Materials Science University of Milano-Bicocca U5, Via Roberto Cozzi 55, 20125, Milano (Italy)

[c] Institute for Photonics and Nanotechnologies-CNR, Via alla Cascata 56/C, 38123 Povo (TN), Italy.

[+] the authors have equally contributed to the manuscript

* e-mail: m.muhyuddin@campus.unimib.it

** e-mail: lior.elbaz@biu.ac.il

Table S1. The electrocatalysts obtained at different levels of experimental design

Sample Labeling	Fe carrying Functionalization of SiO_2 Templating Agent	Organic Precursor	First Pyrolysis (P1)	Acid wash (P1A)	Second Pyrolysis (P1AP2)
SAFe_M_P1	APTES	Methylimidazole	✓		
SAFe_M_P1A	APTES	Methylimidazole	✓	✓	
SAFe_M_P1AP2	APTES	Methylimidazole	✓	✓	✓
SEFe_M_P1	EDTMS	Methylimidazole	✓		
SEFe_M_P1A	EDTMS	Methylimidazole	✓	✓	
SEFe_M_P1AP2	EDTMS	Methylimidazole	✓	✓	✓

TGA and ATR-FTIR measurements on functionalized SiO_2 NPs

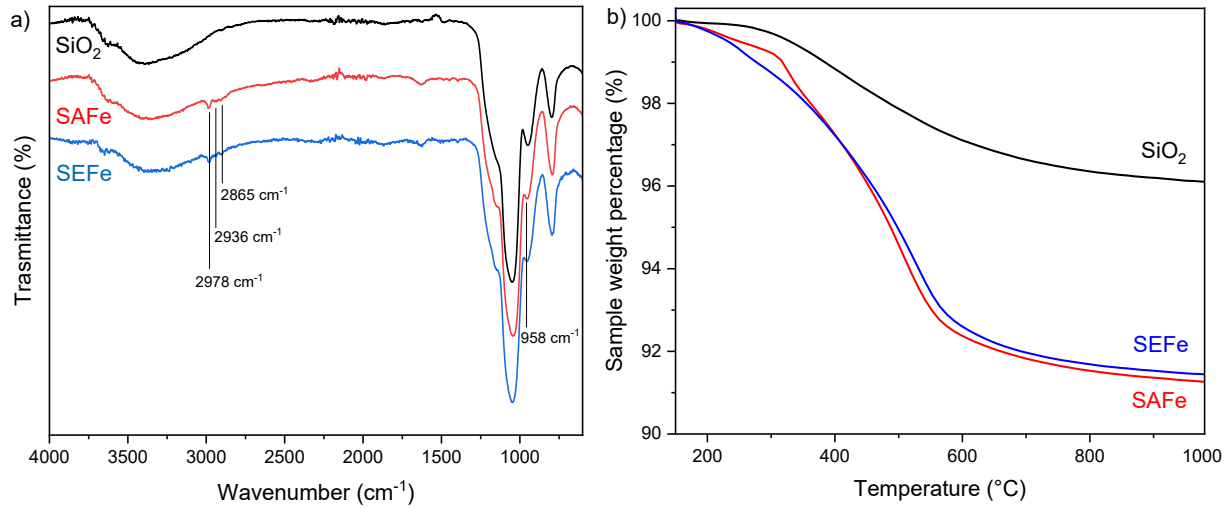

Figure S1. FTIR spectra (a) and TGA curves (b) measured on SAFe and SEFe samples.

ATR-FTIR spectra of SAFe and SEFe (a) show the presence of additional peaks at 2865, 2936 and 2978 cm^{-1} compared to bare SiO_2. These can be possibly attributed to the symmetric and asymmetric stretching of -CH_2 groups of the propyl chains of APTES and EDTMS and to the amino groups of the amino-based ligands, respectively, in agreement with the current literature.[1, 2] Besides, the peak at 958 cm^{-1} due to Si-O-H stretching of surface silanols is shifted at higher wavenumbers in SAFe and SEFe samples compared to bare SiO_2, as a consequence of the partial -OH substitution with the organic ligands and the higher surface disorder. [3, 4]

The TGA curves of both SAFe and SEFe evidence a higher weight loss compared to the bare SiO_2 NPs, due to the additional presence of organic ligands onto the silica surface (Figure S1b). According to our previous work,[5] the weight loss of SiO_2 NPs in the range 150-1000°C ($\Delta W_{150\text{-}1000°C}$) can be attributed to three different contributions:

- The combustion of the organic ligands anchored on SiO_2 NPs due to APTES and EDTMS;
- The water desorption from the surface silanol groups that did not react with APTES and EDTMS, considering that each surface ligand is bonded to silica through two covalent bonds;
- Hydrolysis of the third hydroxy groups of each APTES and EDTMS ligand not involved in bonding on the silica surface.

On this basis, the $\Delta W_{150\text{-}1000°C}$ can be expressed with the following equation:

$$\Delta W_{150-1000°C} = n_R \cdot MW_R + \frac{1}{2} \cdot \left(n_{OH} \cdot w_{SiO_2(1000°C)} - 2n_R\right) \cdot MW_{H_2O} + \frac{1}{2} \cdot n_{OH-APTES} \cdot MW_{H_2O}$$

where n_R is the number of moles of APTES or EDTMS, MW_R is the weight loss of the organic ligand (considering only the organic residue that is bonded to the silica surface), n_{OH} is the moles of surface OH groups per gram of SiO_2 (equal to 5.0 mmol g^{-1}), $w_{SiO2(1000°C)}$ is the weight of SiO_2 measured at 1000°C, MW_{H2O} is the molecular weight of water and $n_{OH\text{-}APTES}$ is the number of moles of hydrolyzed OH groups bonded to APTES or EDTMS molecules that did not react with the surface silanol groups on silica.

From this equation n_R was derived and the amount of APTES and EDTMS anchored to silica (wt%) calculated as:

$$w\%_A = \frac{n_R * MW_R}{m_{SiO2\ (1000°C)}} \times 100$$

According to this equation, the amount of the two ligands on SAFe and SEFe samples was 6.4 ± 0.3 wt% and 5.9 ± 0.2 wt%, respectively.

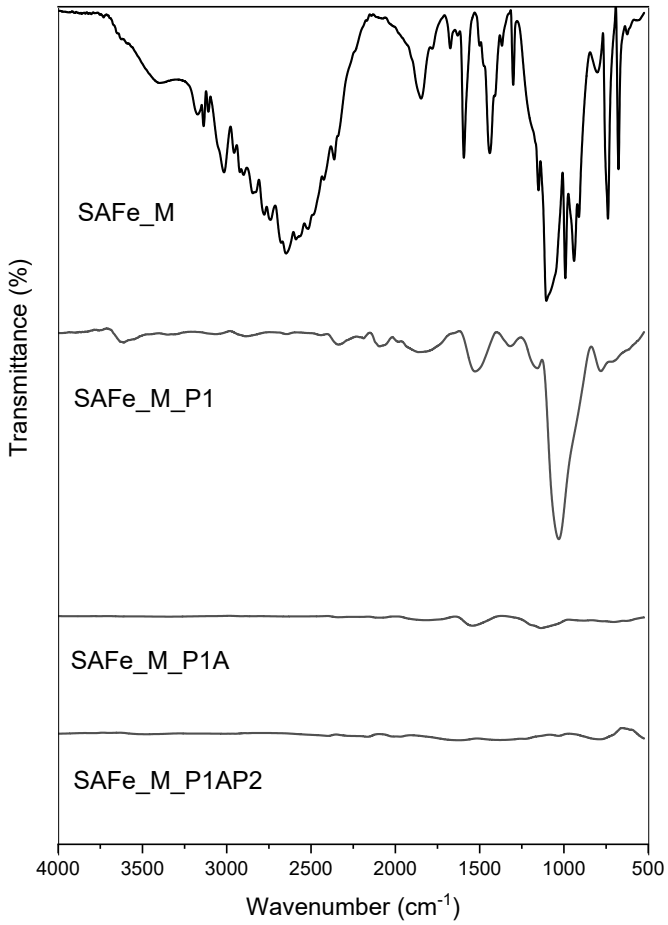

Figure S2. FTIR spectra of SAFe samples mixed with 1-methyimidazole after each preparation step.

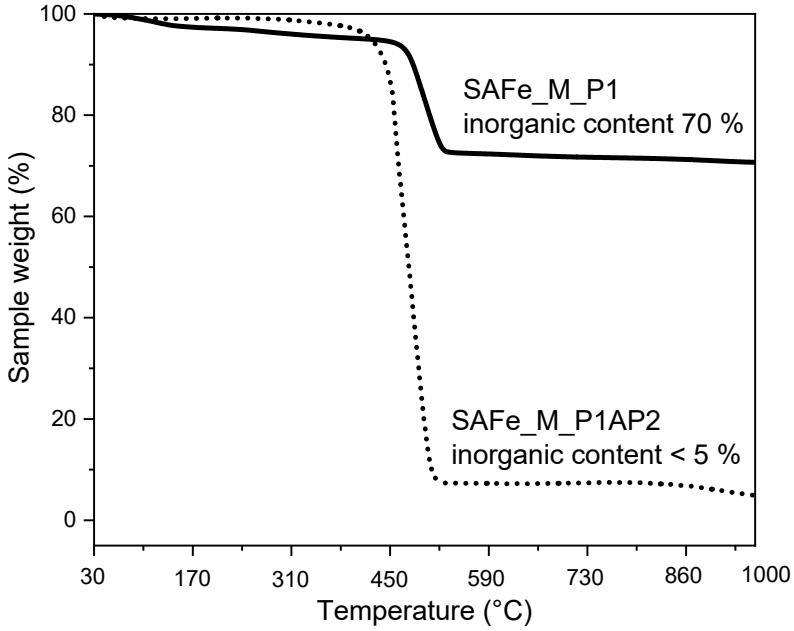

Figure S3. TGA curves measured before and after the silica etching of SAFe chosen as a representative sample.

Table S2. Surface composition estimated by XPS analysis (at.%)

Sample	Carbon	Oxygen	Silicon	Iron	Nitrogen
SEFe	24.43	49.54	18.97	2.08	4.99
SEFe_M	44.46	36.78	14.00	1.11	3.64
SEFe_M_P1	42.58	34.78	18.79	0.64	3.21
SEFe_M_P1A	79.74	11.37	0.39	0.40	8.11
SEFe_MP1AP2	88.98	4.97	-	0.53	5.52
SAFe	23.56	49.92	20.46	1.89	4.17
SAFe_M	38.22	40.69	16.40	1.20	3.49
SAFe_M_P1	78.20	10.83	3.59	0.54	6.85
SAFe_M_P1A	82.43	8.33	0.42	0.42	8.41
SAFe_MP1AP2	88.82	6.76	-	0.33	4.09

Table S3. Iron amounts measured by ICP-OES analysis.

Sample	Iron amount (wt%) by ICP
SAFe	1.4 ± 0.1
SAFe_MP1AP2	0.61 ± 0.08
SEFe	1.5 ± 0.1
SEFe_MP1AP2	0.50 ± 0.09

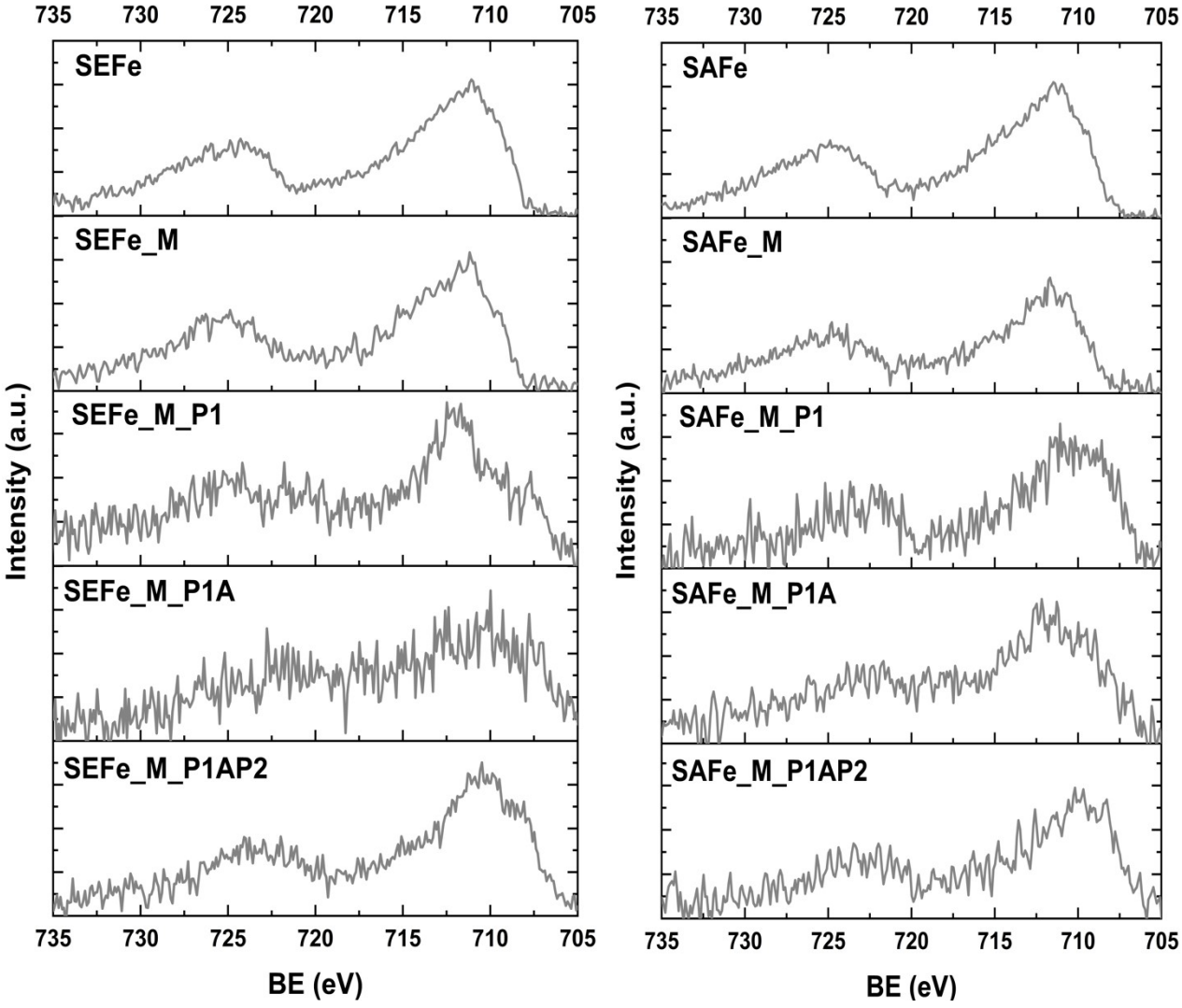

Figure S4. XPS high-resolution Fe2p spectra of (left) SEFe and (Right) SAFe after each preparation step.

Figure S4. shows that both materials have low iron content due to their weak Fe2p spectra, consistent with ICP-OES measurements (< 2 wt% iron, Table S3). Early pyrolysis (P1) alters iron coordination, with $Fe2p_{3/2}$ signals at ~711 eV indicating more Fe^{2+} sites. SAFe_M_P1 and SAFe_M_P1AP2 have similar Fe^{2+} and Fe^{3+} sites, while SEFe_M_P1 retains its original coordination, unlike the final product where Fe^{2+} and Fe^{3+} levels are similar. N1s spectra confirm these findings (Figure 5).

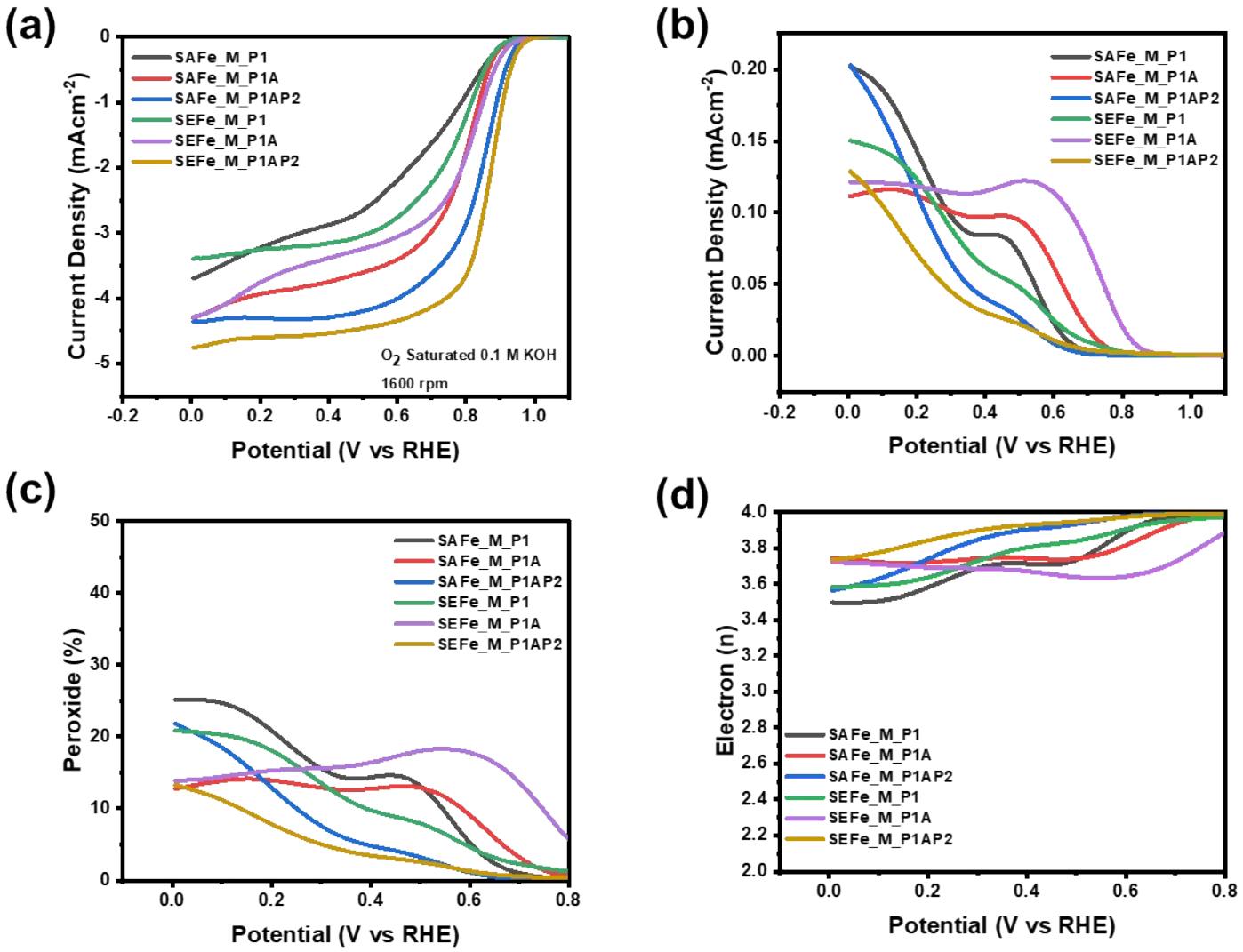

Figure S5. ORR measurements in alkaline media (O_2 rich 0.1 M KOH) demonstrated by electrocatalysts evolved at different stages of the research design while keeping the electrocatalyst loading at 0.6 mg cm^{-2} and rotation of RRDE at 1600 rpm. LSVs obtained at 5mVs^{-1} (a,b), ring current densities (c,d), peroxide yield (e,f) and number of electrons transferred (g,h) during ORR.

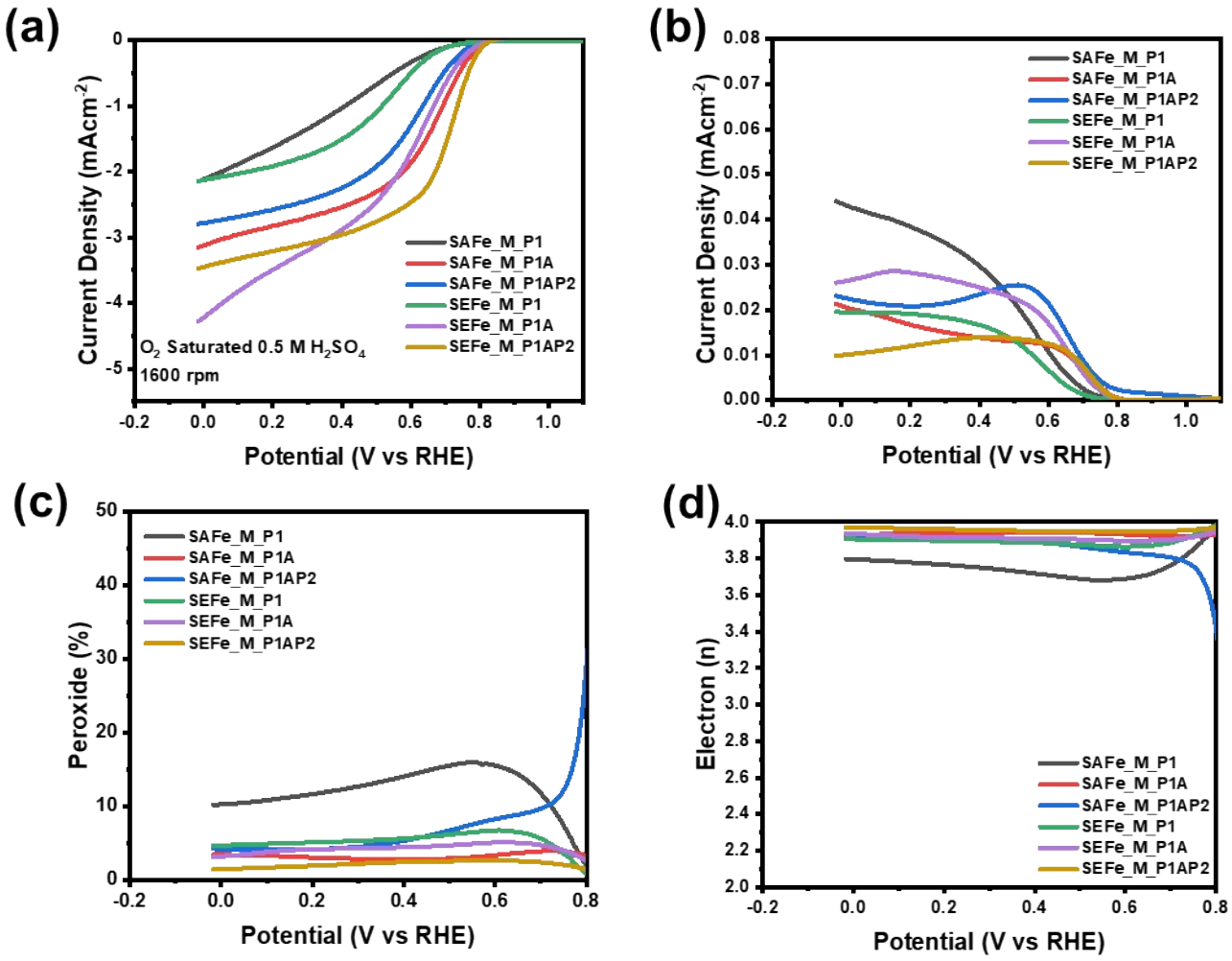

Figure S6. ORR measurements in Acidic media (O_2 rich 0.5 M H_2SO_4) demonstrated by electrocatalysts evolved at different stages of the research design while keeping the electrocatalyst loading at 0.6 mg cm^{-2} and rotation of RRDE at 1600 rpm. LSVs obtained at 5mVs^{-1} (a,b), ring current densities (c,d), peroxide yield (e,f) and number of electrons transferred (g,h) during ORR

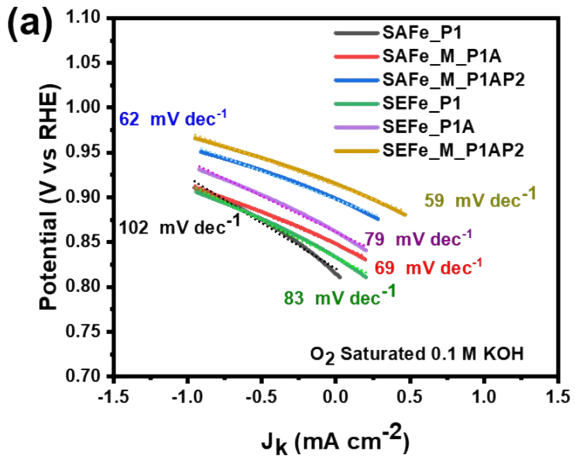

Figure S7. Tafel slopes were evaluated from the RRDE measurements both in 0.1M KOH, according to the equation:

$$J_k = \frac{J_{disk}\, x\, J_{limiting}}{J_{disk} - J_{limiting}}$$

The Tafel slope decreased with each development stage for both electrocatalysts, indicating more favorable kinetics that were attributable to the synthesis approach.

Table S4. Summary of activity and kinetics parameters of SXFe_M electrocatalysts:

Samples	Alkaline Media 0.1 M KOH			Acidic Media 0.5 M H_2SO_4	
	Onset Potential (mV)	Half-Wave Potential (mV)	Tafel slope (mV dec^{-1})	Onset Potential (mV)	Half-Wave Potential (mV)
SAFe_M_P1	910	805	102	707	503
SAFe_M_P1A	910	820	69	792	693
SAFe_M_P1AP2	**950**	**865**	**62**	**772**	**643**
SEFe_M_P1	905	805	83	708	560
SEFe_M_P1A	930	835	79	787	653
SEFe_M_P1AP2	**965**	**880**	**59**	**808**	**723**

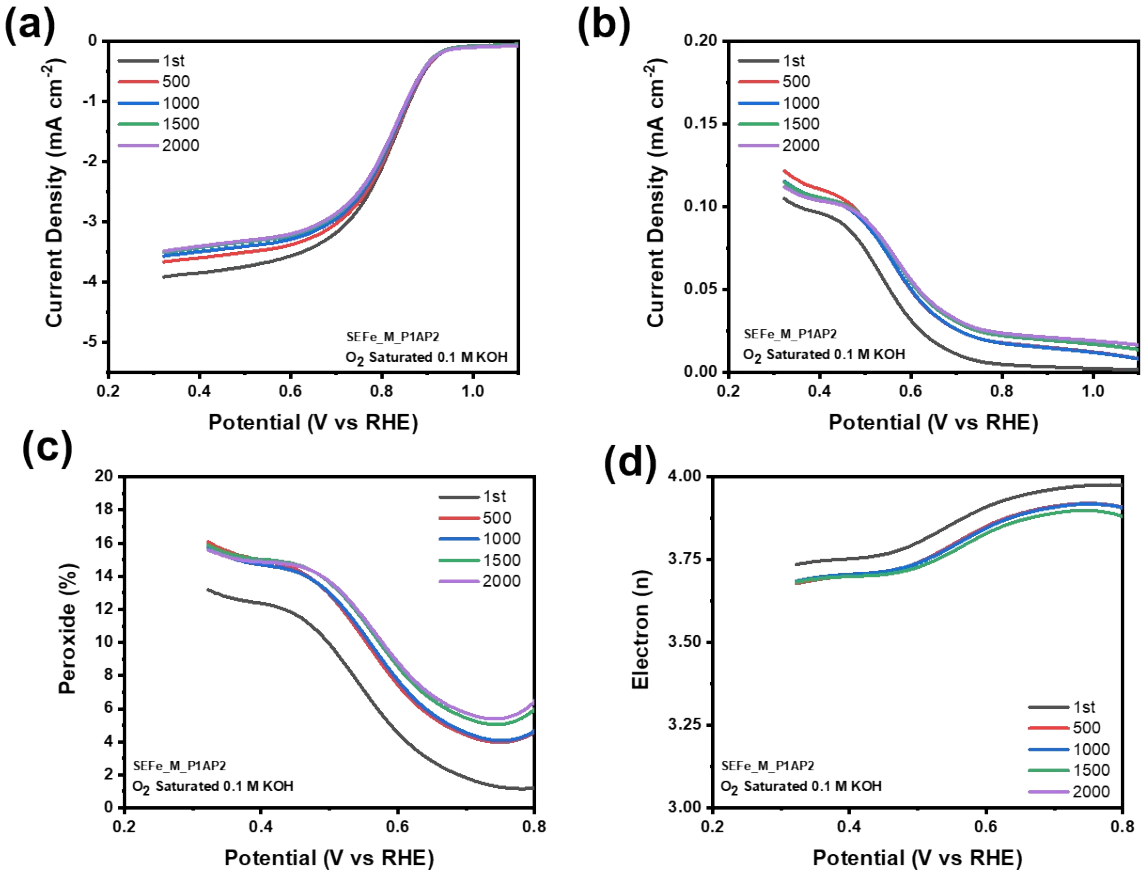

Figure S8. SEFe_M_P1AP2 stability measurement in 0.1M KOH. The measurement was conducted over 2000 cycles at 50mV s^{-2}. The LSV scan rate was 5 mV s^{-2},and recorded after every 500 cycles.

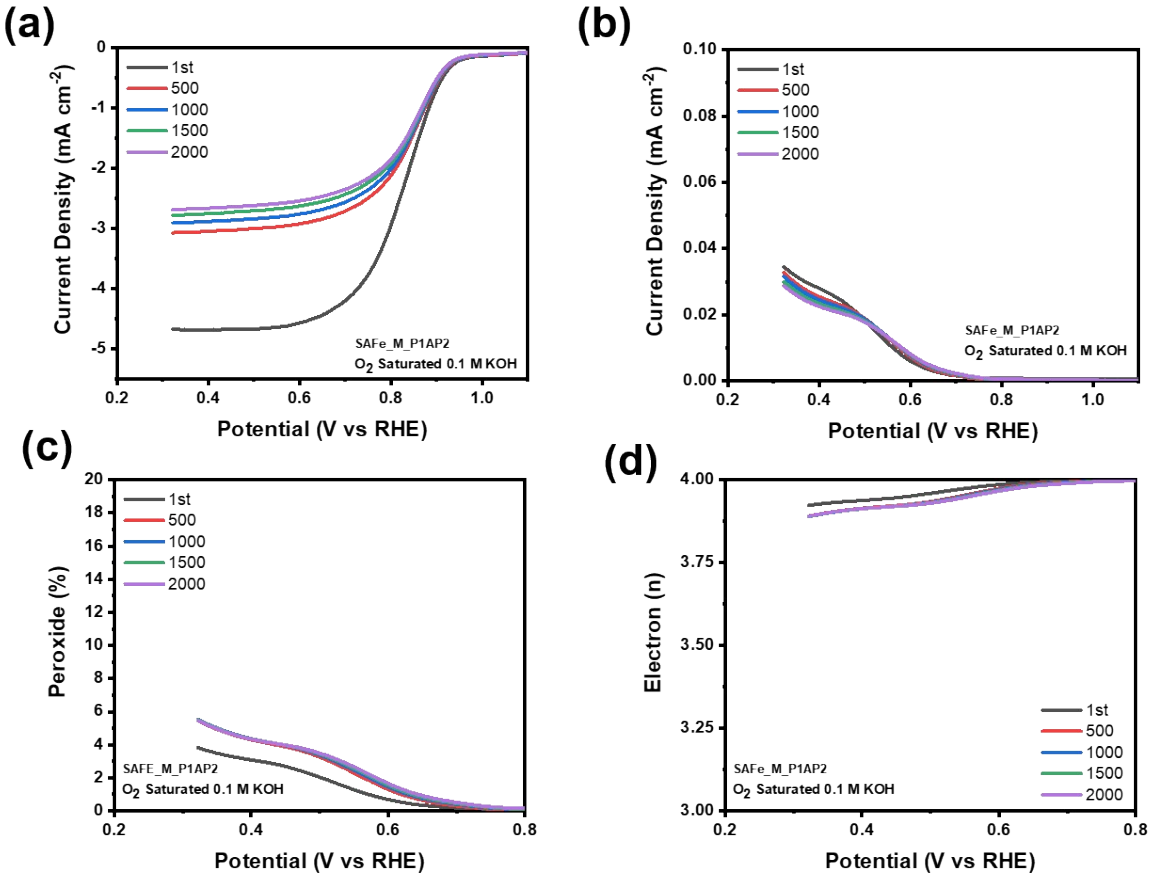

Figure S9. SAFe_M_P1AP2 stability measurement in 0.1M KOH. The measurement was conducted over 2000 cycles at 50mV s^{-2}. The LSV scan rate was 5 mV s^{-2}, and recorded after every 500 cycles.

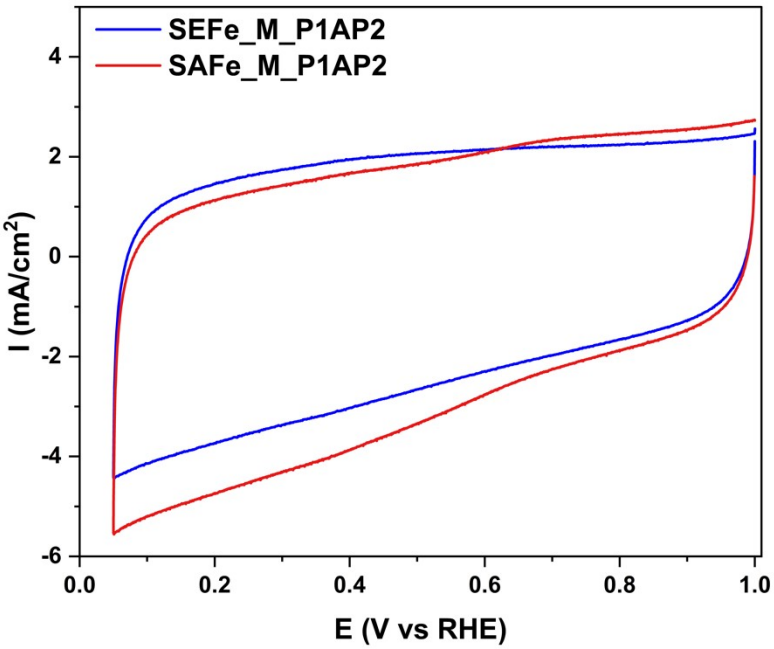

Figure S10. CV of SXFe_M_P1AP2 in AEM fuel cell.

The anode (H_2) and cathode (IV-O_2; CV-N_2) gasses were humidified to 100% RH (60 °C/60 °C/60 °C). The H_2 flow at the anode was 0.3 L min^{-1} and the N_2 flow at the cathode was 0.5 L min^{-1}. The backpressure was 150KPa. The catalysts loading were ~2 mg cm^{-2} at the cathode and 0.6 mg_{Pt} cm^{-2} at the anode.

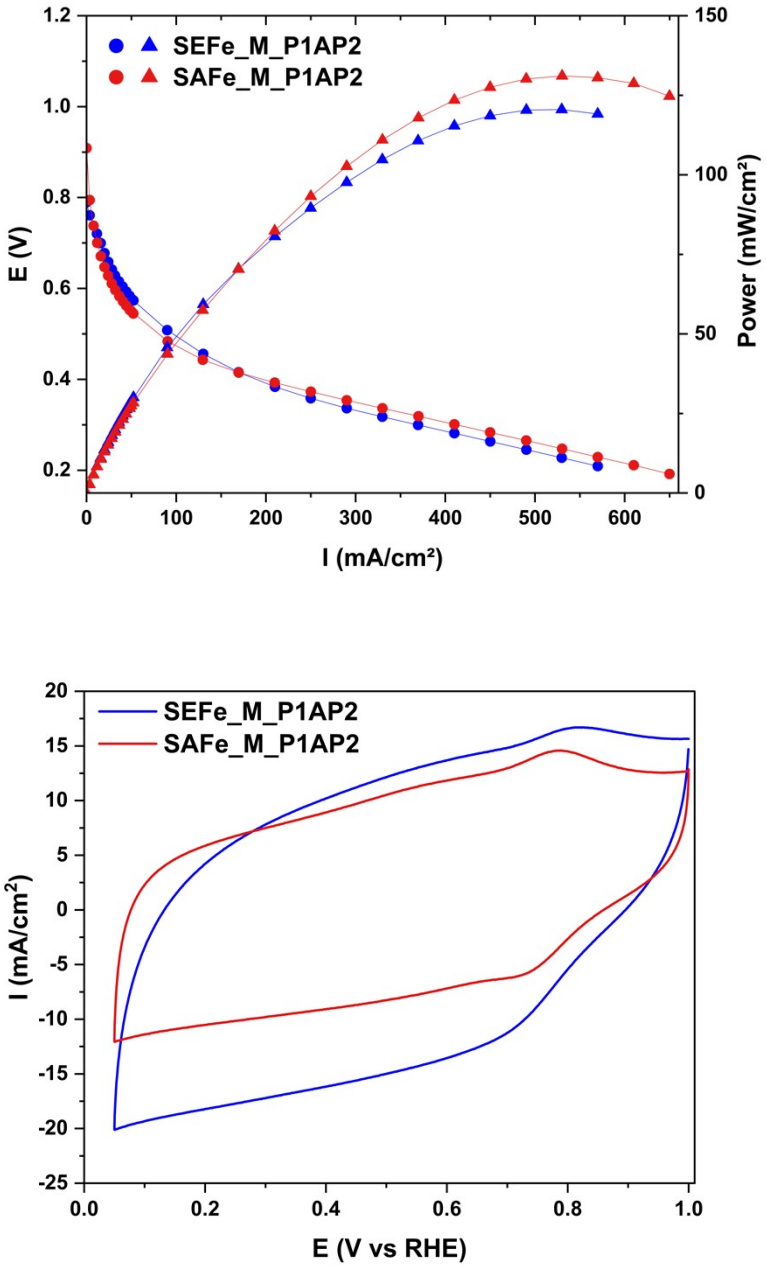

Figure S11. IV curve (top) and CV (bottom) of SXFe_M_P1AP2 in PEM fuel cell.

The anode (H_2) and cathode (IV-O_2; CV-N_2) gasses were humidified to 100% RH (80 °C/80 °C/80 °C). The gasses flow was 0.5 L min^{-1} and the backpressure was 150KPa. The catalysts loading were 0.2mg_{Pt} cm^{-2} and ~5 mg cm^{-2} at the anode and cathode, respectively.

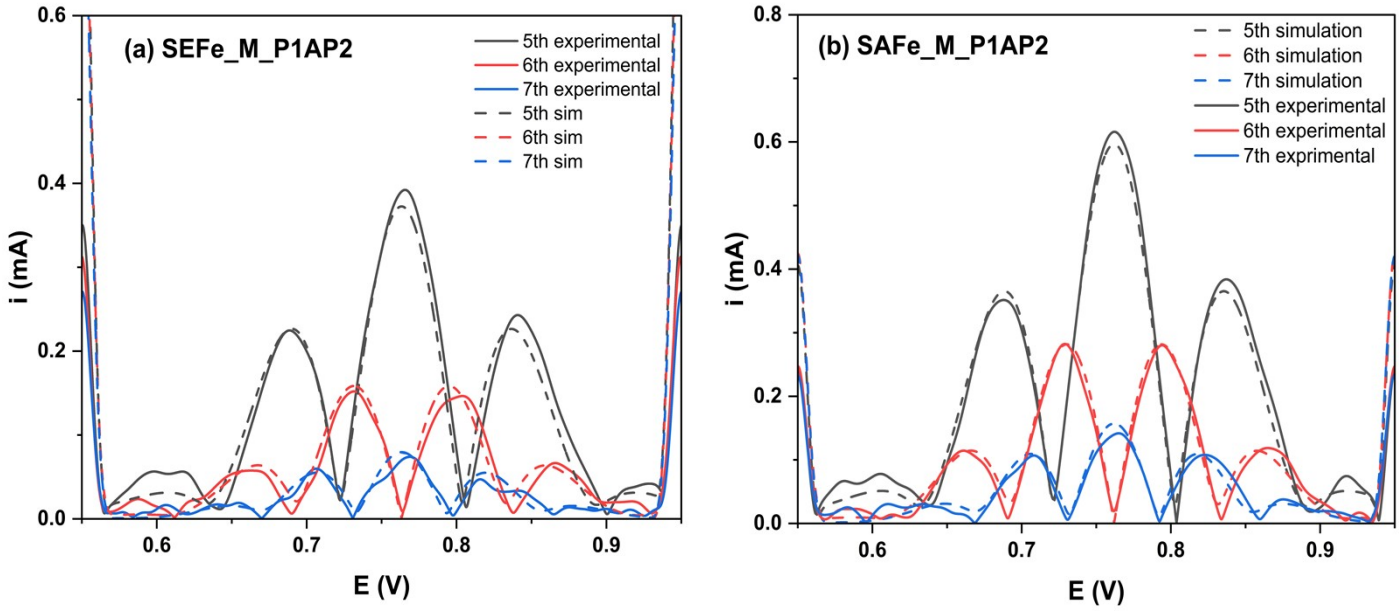

Figure S12. Experimental (solid) and simulated (dashed) fifth, sixth and seventh harmonics extracted from a single FTACV measurement of PEM fuel cell, under the conditions described in figure S11.

ACV parameters: E_i= 0.55V; E_f=0.95V; frequency of the sine wave: f=0.119Hz; amplitude of the sine wave ΔE=110mV; time step for data acquisition Δt=0.8mSec.

Simulation parameters for (a) SEFe_M_P1AP2: R = 0.333 Ohm; Cdl = 0.139 F cm^{-2}; number of sites = $5.72*10^{16}$; E_0 = 0.76; k = 7.88 s^{-1}; C= $1.9*10^{-8}$mol cm^{-2}.

Simulation parameters for (b) SAFe_M_P1AP2: R = 0.144 Ohm; Cdl = 0.09 F cm^{-2}; number of sites = $6.62*10^{16}$; E_0 =0.76 k=6.97 s^{-1}; C = $2.2*10^{-8}$mol cm^{-2}.

References

1. Chiang, C.-H.; Ishida, H.; Koenig, J. L., The structure of γ-aminopropyltriethoxysilane on glass surfaces. *Journal of Colloid and Interface Science* **1980,** *74* (2), 396-404.
2. Culler, S.; Ishida, H.; Koenig, J., Structure of silane coupling agents adsorbed on silicon powder. *Journal of colloid and interface science* **1985,** *106* (2), 334-346.
3. Morrow, B.; McFarlan, A., Surface vibrational modes of silanol groups on silica. *The Journal of Physical Chemistry* **1992,** *96* (3), 1395-1400.
4. Morrow, B.; McFarlane, R. A., Trimethylgallium adsorbed on silica and its reaction with phosphine, arsine, and hydrogen chloride: an infrared and Raman study. *The Journal of Physical Chemistry* **1986,** *90* (14), 3192-3197.
5. Mostoni, S.; D'Arienzo, M.; Di Credico, B.; Armelao, L.; Rancan, M.; Dirè, S.; Callone, E.; Donetti, R.; Susanna, A.; Scotti, R., Design of a Zn Single-Site Curing Activator for a More Sustainable Sulfur Cross-Link Formation in Rubber. *Industrial & Engineering Chemistry Research* **2021,** *60* (28), 10180-10192.